Mikrochim. Acta 135, 63–69 (2000)

Mikrochimica Acta
© Springer-Verlag 2000
Printed in Austria

Physicochemical Properties of Plant Protection Substances: I Polymorphism and Binary Systems of Triadimenol*

Artur Burger** and **Christian van den Boom**

Department of Pharmacognosy, University of Innsbruck, Josef-Moeller-Haus, Innrain 52, A-6020 Innsbruck, Austria

Abstract. The fungicide triadimenol consists of a mixture of two diastereoisomers. Diastereoisomer A (1*RS*,2*SR*) could be obtained from the mixture by fractionated crystallization from ethanol/water and toluene, successively, whereas diastereoisomer B (1*RS*,2*RS*) could be separated by column chromatography on a silica gel column using ethylacetate as eluent. Four different crystal forms of diastereoisomer A could be derived. The modifications were characterized by means of thermal analysis (thermomicroscopy, DSC), FTIR-spectroscopy, FT-Raman-spectroscopy and powder X-ray diffraction, as well as pycnometry. The thermodynamic relationships are illustrated in a semi-schematic energy/temperature-diagram which provides information about the relative thermodynamic stabilities and physical properties of the four crystal forms. Mod. II (m.p. 132 °C, ΔH_f 33.1 ± 0.2 kJ · mol^{-1}, density 1.271 ± 0.001 g · cm^{-3}) was obtained from toluene after the separation of diastereoisomer A and is enantiotropically related to mod. I (m.p. 138 °C, ΔH_f 32.0 ± 0.2 kJ · mol^{-1}, density 1.243 ± 0.001 g · cm^{-3}). The transition point of mod. II with mod. I was determined between 30 and 40 °C, which means that mod. II is thermodynamically stable at ambient conditions. Mod. III (m.p. 112 °C, ΔH_f 25.1 ± 0.5 kJ · mol^{-1}) and mod. IV were obtained from the melt. Furthermore, the phase diagrams of the binary systems of diastereoisomer B and the four modifications of diastereoisomer A were calculated by means of the experimentally obtained thermodynamical data.

Key words: Triadimenol; thermal analysis; polymorphism; energy/temperature-diagram; binary system; separation of diastereoisomers.

Triadimenol [(1*RS*,2*RS*;1*RS*,2*SR*)-1-(4-Chlorophenoxy)-3.3-dimethyl-1-(1*H*-1.2.4-triazol-1-yl)-butan-2-ol)] is an agricultural fungicide systemically active against powdery mildews and rusts of grains. Similar to pharmaceutically used triazine-antimycotics, the mode of action is based on the inhibition of the ergosterol biosynthesis. Because of the two chirality centers at the asymmetric carbon atoms C_1 and C_2, four stereoisomers of triadimenol exist (Fig. 1). Commercial products are made of a mixture of two diastereoisomers. The ratio of diastereoisomer A (1*RS*,2*SR*) to diastereoisomer B (1*RS*,2*RS*) is approximately 70:30 [1].

The variety of melting points of triadimenol published in the literature so far shows, that neither stereochemistry nor polymorphism has been considered as yet. Table 1 gives a survey of significant reference-books and articles in which melting points of triadimenol are reported.

Experimental

Material

The studies were carried out using triadimenol "Reference Standard" provided by Bayer AG (Germany). According to GLC determinations performed by Bayer AG, the ratio of diastereoisomer A to diastereoisomer B comes to 79:19.3. The purity was 98.3%.

Thermoanalytical Methods

Polarization thermomicroscopy was performed using a Kofler hot stage microscope (Thermovar®, Reichert, Vienna, Austria). To

* Part of this work was presented at the 4th Symposium/Workshops on Pharmacy and Thermal Analysis, Karlsruhe, Germany, March 23–26, 1999

** To whom correspondence should be addressed

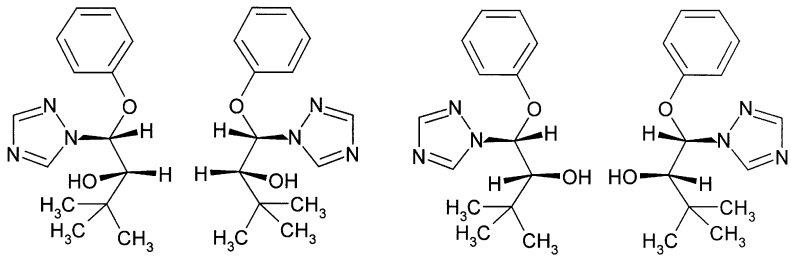

Fig. 1. Stereoisomers of triadimenol

Table 1. Survey of reference-books and articles in which melting points of triadimenol are reported

Author/editor	Compound as named by the author/editor	Melting point/ melting range
Tomlin [1]	diastereoisomer A	138.2 °C
Tomlin [1]	diastereoisomer B	133.5 °C
Tomlin [1]	eutectic temperature of diastereoisomer A and diastereoisomer B	110 °C
Gasteiger and Kaufmann [9]	diastereoisomer A	132 °C
Frohberger [10]	β-form	112 °C
Budavari [11]	β-form	112–117 °C
Falbe and Regitz [12]	1*RS*,2*RS*,1*RS*,2*SR*	138.2 °C

prepare a crystal film, ca. 2 mg of triadimenol were heated between a microscope slide and a cover glass using a Kofler hot bench (Reichert, Vienna, Austria) [2].

Differential scanning calorimetry (DSC) was carried out with a DSC-7 and Pyris software for Windows NT (Perkin-Elmer, Norwalk, Ct., USA) using aluminum sample-pans (25 µL). Sample masses for quantitative analysis were 1–3 ($\pm$0.0005) mg (Ultramicroscales UM3, Mettler, CH-Greifensee, Switzerland). Nitrogen 99.999% (20 ml · min^{-1}) was used as purge gas. Calibration of the temperature axis was carried out with benzophenone (m.p. 48.0 °C) and caffeine (m.p. 236.2 °C). Enthalpy calibration of the DSC signal was performed with indium 99.999% (Perkin-Elmer, Norwalk, Ct., USA). The usual heating rate was 5 K · min^{-1}.

Spectroscopic Methods

FTIR-spectra were recorded with a Bruker IFS 25 FTIR-spectrometer (Bruker Analytische Meßtechnik GmbH, Karlsruhe, Germany) connected to a Bruker FTIR-microscope (15×Cassegrain-objective and visible polarization). Samples were scanned as potassium bromide pellets at an instrument resolution of 2 cm^{-1} (50 interferograms, internal mode). For recording microscope spectra, a crystal film was prepared between two zinc selenide windows. The spectral resolution is 4 cm^{-1} (focus diameter 50 µm, 100 interferograms).

FT-Raman spectra were recorded with a Bruker RFS 100 FT-Raman spectrometer (Bruker Analytische Meßtechnik GmbH, Karlsruhe, Germany) equipped with a diode pumped 100 Nd:YAG Laser (1064 nm) as excitation source and a liquid nitrogen-cooled high-sensitivity Ge-detector (64 scans at 4 cm^{-1} instrument resolution).

Powder X-ray Diffraction

X-ray powder diffraction patterns were obtained on a Siemens D-5000 X-ray diffractometer equipped with Θ/Θ-goniometer (Siemens AG, Karlsruhe, Germany) using monochromatic CuK_α radiation (tube voltage 40 kV, tube current 40 mA) from 2 to 40° 2Θ at a rate of 0.005° 2Θ s^{-1}. The diffractometer was fitted with a Göbel mirror and a scintillation counter.

Pycnometry

The determination of the powder volumes were carried out by means of an air comparison pycnometer (Ultrapycnometer 1000, Quantachrome Corp., Syosset, N.Y., USA) provided with a small sample cell at 25 °C. The samples (1 $\pm$ 0.0005 g) were purged with helium for 15 min. Calibration was carried out with a steel sphere.

Results

Separation of the Triadimenol Diastereoisomers

The DSC-curve of the triadimenol reference standard (Fig. 2) shows the typical pattern of a simple eutectic

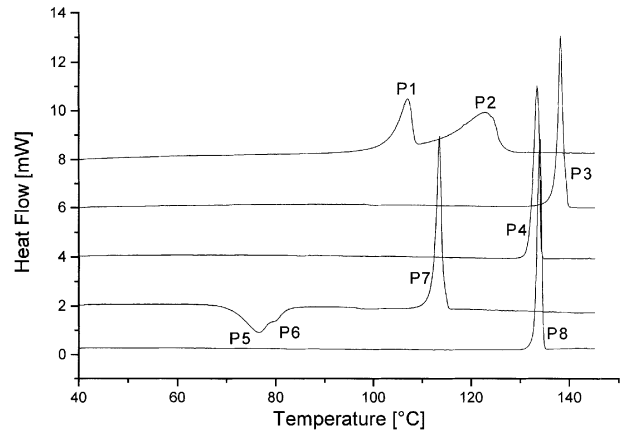

Fig. 2. DSC-curves of triadimenol (see text)

Table 2. Calculated and thermomicroscopically determined eutectic temperatures (ET) within the binary systems of the crystal forms of the diastereoisomers A and B

Components	Calculated ET [°C]	Mole fraction at ET	Thermomicroscopically determined ET [°C]
Diastereoisomer A mod. I and diastereoisomer B	107.8	0.48	109
Diastereoisomer A mod. II and diastereoisomer B	106.4	0.51	107
Diastereoisomer A mod. III and diastereoisomer B	92.6	0.67	95

system in which the liquid phases are miscible with each other in all proportions but the components form neither compounds nor mixed crystals. The first peak corresponds to the eutectic temperature (P1). The second peak shows the melting process of diastereoisomer A (P2) which is present in excess in the mixture.

For separating the diastereoisomers the following procedures have been developed.

Diastereoisomer A. 30 g of the triadimenol reference standard were dissolved in 400 mL ethanol (70% V/V) at 50 °C. After that, 150 mL of ethanol were evaporated in vacuum (200 mbar). The crystals growing when cooling the solution at 15 °C for 2 h were filtered and in the following crystallized twice from toluene.

Diastereoisomer B. 5 mL of a solution of the triadimenol reference standard in ethylacetate (8% m/m) were chromatographed on a silica gel column using ethylacetate as eluent. The fractions containing only diastereoisomer B were combined and the solvent was evaporated in vacuum. Final purification was carried out by crystallization from toluene at 15 °C.

Preparation of the Modifications

When separating diastereoisomer A from the mixture of both diastereoisomers as described above, white crystals of diastereoisomer A mod. II are obtained. Mod. I can easily be obtained by stirring (magnetic stirrer) a suspension of diastereoisomer A mod. II for 24 h in n-hexane at 50 °C. To exclude kinetic retardation, a few drops of acetone were added. Mod. III and mod. IV of diastereoisomer A can be crystallized from the melt. When quenching a molten crystal film on a metal cooling block, the melt fails to crystallize at first. After slowly heating the amorphous phase on the thermomicroscope or in the DSC respectively, mod. IV crystallizes at 60 °C and is successively transformed to mod. III between 75 and 80 °C.

Diastereoisomer B was found to crystallize only in one crystal form.

The physicochemical properties of all four crystal forms of diastereoisomer A and of diastereoisomer B are summarized in Table 3.

Thermomicroscopy

The equilibrium melting point [3] of diastereoisomer A mod. II is 133 °C. If crystals of diastereoisomer A mod. II are heated slowly, inhomogeneous melting might be detected, which means, that rod-shaped crystals of diastereoisomer A mod. I crystallize from the melt of diastereoisomer A mod. II. Diastereoisomer A mod. I melts at 138 °C. As described above, when quenching a molten crystal film on a metal cooling block, the melt fails to crystallize at first. When slowly heating the amorphous phase on the thermomicroscope or in the DSC, respectively, the crystallization of diastereoisomer A mod. IV building small spherulites in the crystal film can be observed at 60 °C. Between 75 and 80 °C the transition of diastereoisomer A mod. IV into diastereoisomer A mod. III takes place. This transition is very difficult to discover even in polarized light because it is not accompanied with an evident change of polarization colours but only with a darkening of the whole crystal film. On further heating diastereoisomer A mod. III melts at 112 °C. When heating very slow, growth of diastereoisomer A mod. I forming large plates can be observed in the crystal film. In some cases, even inhomogeneous melting of diastereoisomer A mod. III could be observed, in the course of which diastereoisomer A mod. I as well as mod. II have been observed to crystallize from the melt of mod. III.

Diastereoisomer B melts at 133 °C (equilibrium melting point). No further crystal form could be derived from the melt.

Differential Scanning Calorimetry

The DSC-curves of diastereoisomer A mods. I, II, III, IV and of diastereoisomer B are shown in Fig. 2. P3, P4 and P8 correspond to the melting peaks of diastereo-

Table 3. Thermodynamic parameters of the four crystal forms of diastereoisomer A and of diastereoisomer B

Diastereoisomer Modification	A I	A II	A III	A IV	B
M.p. [°C] TM	138	133	112		133
M.p. [°C] DSC	138	132	112		133
Enthalpy of fusion $[kJ \cdot mol^{-1}] \pm 95\%$-c.i.	32.0 ± 0.2	33.1 ± 0.2	25.1 ± 0.5		33.2 ± 0.3
Entropy of fusion $[J \cdot K^{-1} \cdot mol^{-1}] \pm 95\%$-c.i.	78.0 ± 0.4	81.6 ± 0.6	65.2 ± 1.3		81.7 ± 0.7
Thermodynamic transition point [°C] *into mod. I* (calculated[a])		30–40 (44)			
Transition temperature (TM) [°C]			from 60 (→II)	75–82 (→III)	
True density $[g \cdot cm^{-3}] \pm 95\%$-c.i.	1.243 ± 0.001	1.271 ± 0.001			1.312[b]
Thermodynamic stability[c] at 25 °C	b	a	c	d	
1st IR-Peak [cm^{-1}]	3237	3343[d]	3252		3242
Eutectic temperature (TM) [°C] with diastereoisomer B (calculated[e])	109 (108)	107 (106)	95 (93)		

[a] According to Yu [13] and Burger and Henck [14].
[b] Calculated from single crystal data in [4] by means of the program *PowderCell* [15].
[c] a: stable, b: less stable ....
[d] Exception to the Infrared Rule [16].
[e] By means of the equation of Schroeder-Van Laar [5].

isomer A mod. I and II and of diastereoisomer B. The melting points of diastereoisomer A mod. II and diastereoisomer B are remarkably similar. The DSC-curve of diastereoisomer A mod. III primarily shows an exothermic peak which corresponds to the crystallization of diastereoisomer A mod. IV from the melt (P5). This peak is overlapped by a second exothermic peak which corresponds to the transition of diastereoisomer A mod. IV into diastereoisomer A mod. III (P6). Due to this transition it is not possible to determine the melting point of diastereoisomer A mod. IV. Nevertheless, it becomes evident from this transition, that diastereoisomer A mod. IV has to have the lowest melting point. Diastereoisomer A mod. III melts homogeneously at 112 °C (P7).

True Density

The true densities of diastereoisomer A mods. I and II determined by gas comparison pycnometry are given

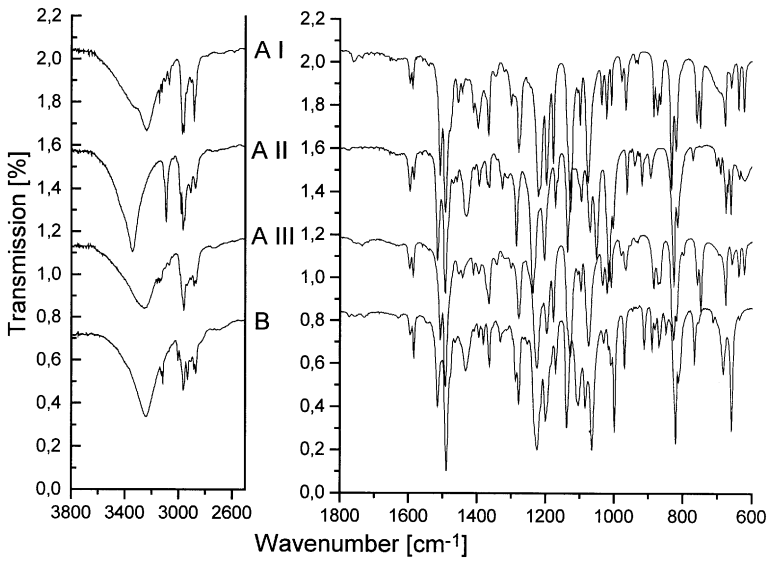

Fig. 3. FTIR-spectra of triadimenol diastereoisomer A mods I (KBr), II (KBr) and III (ZnSe) and of diastereoisomer B (KBr)

in Table 3. The density of diastereoisomer B has been calculated from the single crystal data given in [4].

FTIR Spectroscopy

The FTIR-spectra of diastereoisomer A mods. I and II and of diastereoisomer B (Fig. 3) were recorded using potassium bromide pellets, while the FTIR-spectrum of diastereoisomer A mod. III could only be obtained by temperature-controlled FTIR-microspectroscopy from a crystal film prepared between two zinc selenide windows. The recorded spectra show evident and characteristic differences in the IR-absorption bands in the region from 3260 cm^{-1} to 3230 cm^{-1}, 1520 cm^{-1} to 1505 cm^{-1}, 1280 cm^{-1} to 1030 cm^{-1} and 835 cm^{-1} to 660 cm^{-1}.

FT-Raman Spectroscopy

According to the FTIR-spectra, the FT-Raman-spectra of the three crystal forms of diastereoisomer A also show evident differences in the region from 1380 cm^{-1} to 1120 cm^{-1} (Fig. 4). Additional spectral information is provided by the FT-Raman-spectra as far as the lattice vibrations are concerned. Characteristic differences can be detected in this region from 950 cm^{-1} to 600 cm^{-1}.

Powder X-Ray Diffraction

The X-ray diffraction powder patterns of mod. diastereoisomer A I, II and III (Fig. 5) show clear differences in the d-values and relative intensities. The powder pattern of mod. diastereoisomer A III was directly recorded from a crystal film.

Phase Diagram of the Binary Systems of Diastereoisomer A and Diastereoisomer B

The modifications of diastereoisomer A build a simple eutectic system with diastereoisomer B. Therefore, it is

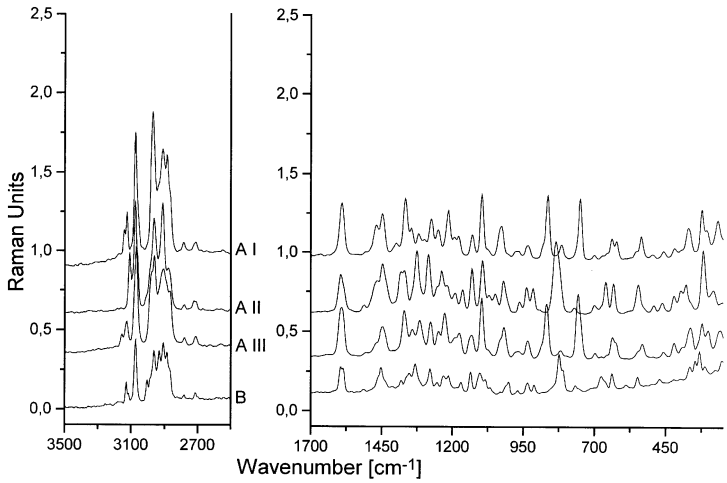

Fig. 4. FT-Raman spectra of triadimenol diastereoisomer A mods. I, II and III and of diastereoisomer B

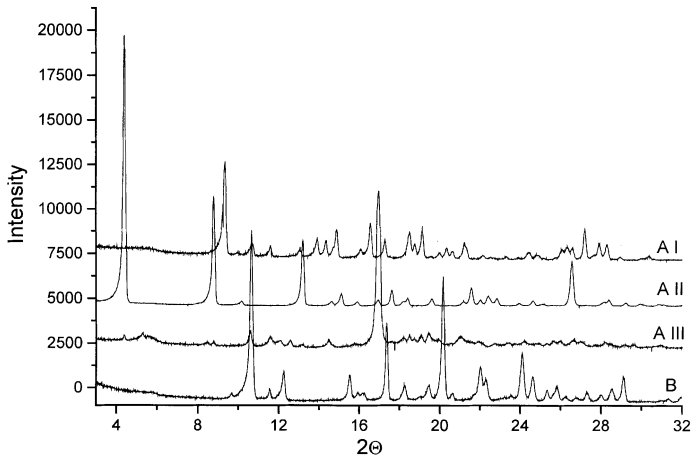

Fig. 5. X-ray powder patterns of triadimenol diastereoisomer A mods. I, II and III and of diastereoisomer B

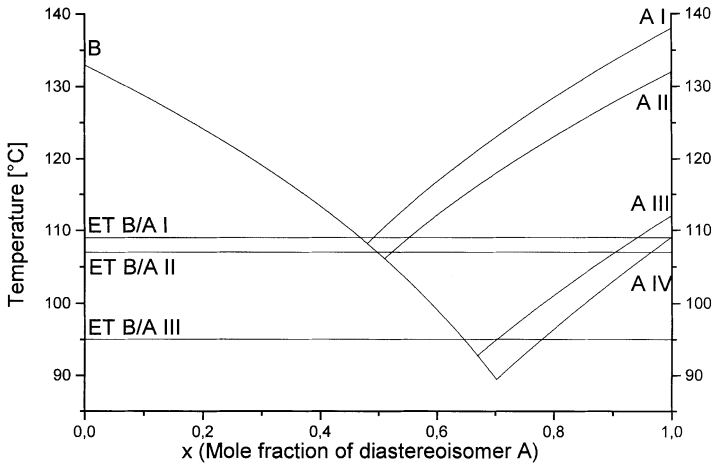

Fig. 6. Phase diagrams of the binary systems of triadimenol diastereoisomer B with the four modifications of diastereoisomer *A* (*A* I *to A* IV); *B, A* I, *A* II *and A* III: calculated liquidus curves, *A* IV: estimated liquidus curve; horizontal lines: eutectic temperatures (measured by thermomicroscopy)

possible to calculate the phase diagrams of the binary systems of mods. I, II and III of diastereoisomer A with diastereoisomer B by means of the equation of Schroeder-Van Laar [5]. By applying the thermodynamic data determined by DSC-investigations, the liquidus curves may be constructed (Fig. 6).

The calculated phase diagrams of Fig. 6 may be verified by thermomicroscopical determination of the eutectic temperatures of the crystal forms of diastereoisomer A with diastereoisomer B. In Fig. 6 the eutectic temperatures thermoanalytically determined are given as horizontal lines; the calculated eutectic temperatures are given by the temperature at which the liquidus curves do intersect. The calculated data were found to be in good agreement with the experimentally determined values (see Table 2).

Thermodynamic Transition Point Between Diastereoisomer A Mod. I and Diastereoisomer A Mod. II

The entropy-of-fusion rule and the density rule [6] indicate an enantiotropic relationship between diastereoisomer A mods. I and II. As it is not possible to detect the endothermic transition from diastereoisomer A mod. II into diastereoisomer A mod. I by DSC, suspensions of diastereoisomer A mods. I and II in n-hexane were stirred by a magnetic stirrer in a water bath at different temperatures [7]. The residue crystals were investigated by FTIR-spectrosopy. The crystal products produced up to 30 °C correspond to mod. II whereas the 40 °C residue crystals were of diastereoisomer A mod. I. Therefore, the thermodynamic transition point lies between 30 and 40 °C.

Discussion

By applying the entropy-of-fusion rule and the density rule [6], it can not only be stated that mods. I and II of diastereoisomer A behave enantiotropically but also that diastereoisomer A mod. III and mod. IV behave monotropically to each other and to I and II. By means of the experimentally determined thermodynamic parameters it is now possible, to establish the semischematic energy/temperature-diagram [6–8] for triadimenol diastereoisomer A, which is depicted in Fig. 7.

There are several reasons responsible for the confusion with the published melting points. First, triadimenol is a binary system which has obviously not been considered by all previous authors. Second, diastereoisomer A exists in four crystal forms of which the highest melting form is not the thermodynamic stable one at room-temperature. Third, the melting points of diastereoisomer B and diastereoisomer A mod. II are both approximately 133 °C. Fourth, the eutectic temperature published so far is quite senseless without stating which modification of diastereoisomer A has been analyzed. And fifth, the melting point of diastereoisomer A mod. III is very similar to the eutectic temperature of diastereoisomer A mod. II/diastereoisomer B. Especially in practice concerning stability and storage conditions, it is further interesting, that all melting points published so far refer to diastereoisomer A mod. I although it is not the crystal form thermodynamically stable at ambient conditions. As triadimenol is agriculturally used as a powder or as a slurry for seed treatment, the analytical aspects as well as the transition temperature of diastereoisomer A mod. I/II at about 35 °C are of practical interest.

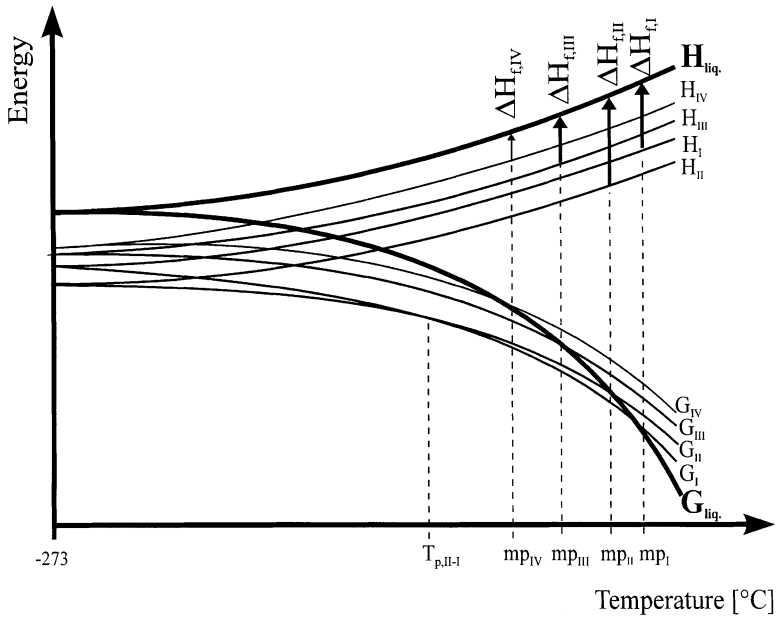

Fig. 7. Semischematic energy/temperature-diagram of the modifications of triadimenol diastereoisomer A (I–IV) and of the melt (liq.); *G* molar free enthalpy, *H* molar enthalpy, ΔH_f heat of fusion, ΔH_t heat of transition, *Tp* thermodynamic transition point. Measured enthalpy effects are bold. Energy axis without scale; Temperature axis enlarged towards higher temperatures. The melting point (*mp*) corresponds to that temperature, at which the $G_{liq.}$-curve and the G-curve intersect

References

[1] C. Tomlin (Ed.) *The Pesticide Manual Incorporating the Agrochemicals Handbook, 10th Edn*. The British Crop Protection Council, Surrey, 1994, p. 1002.

[2] M. Kuhnert-Brandstätter, *Thermomicroscopy of Organic Compounds*. In: G. Svehla (Ed.) Comprehensive Analytical Chemistry, Vol. XVI. Elsevier Scientific Publishing Company Inc., Amsterdam, 1982, pp. 423–425.

[3] L. Kofler, A. Kofler, *Thermo-Mikro-Methoden zur Kennzeichnung organischer Stoffe und Stoffgemische, 3rd Edn*. Verlag Chemie GmbH, Weinheim/Bergstraße, 1954, pp. 17–18.

[4] T. Spitzer, J. Kopf, G. Nickless, *Cryst. Struct. Comm*. **1982**, *11*, 315.

[5] J. Jaques, A. Collet, S. H. Wilen, *Enantiomers, Racemates and Resolutions, 1st Edn*. Wiley, New York, 1981, pp. 44–47.

[6] A. Burger, R. Ramberger, *Mikrochim. Acta* II **1979**, 259.

[7] A. Burger, *Acta Pharm. Technol*. **1982**, *28*, 1.

[8] A. Grunenberg, J.-O. Henck, H. W. Siesler, *Int. J. Pharm*. **1996**, *129*, 147.

[9] J. Gasteiger, K. Kaufmann, *Tetrahedron Lett*. **1985**, *26*, 4341.

[10] P. E. Frohberger, *Pflanzenschutz-Nachrichten Bayer* **1978**, *31*, 11.

[11] S. Budavari (Ed.) *The Merck Index, 12th Edn*. Merck Research Laboratories, Whitehouse Station NJ, 1996, pp. 1636–1637.

[12] J. Falbe, M. Regitz (Ed.) *Römpp Chemie Lexikon, 9th Edn*. Georg Thieme Verlag, Stuttgart, 1992, pp. 4694–4695.

[13] L. Yu, *J. Pharm. Sci*. **1995**, *84*, 966.

[14] A. Burger, J.-O. Henck, *Prediction of the Transition Point of Enantiotropically Related Polymorphic Systems Using Thermodynamical Data, Poster Presentation*. 2nd Symposium/ Workshops on Pharmacy and Thermal Analysis, October 17–19, 1995, Geneve.

[15] W. Kraus, G. Nolze, *PowderCell for Windows Vers. 2.0 Beta*. Program for Manipulation of Crystal Structures and Calculation of X-Ray Powder Patterns. Federal Institute for Materials Research and Testing, Berlin, 1998.

[16] A. Burger, R. Ramberger, *Mikrochim. Acta* II **1979**, 273.

Received September 30, 1999. Revision July 30, 2000.